

Wakefields studies for the SXFEL user facility

Ming-Hao Song^{1,2} · Chao Feng¹ · Da-Zhang Huang¹ · Hai-Xiao Deng¹ · Bo Liu¹ · Dong Wang¹

Received: 3 January 2017 / Revised: 2 March 2017 / Accepted: 19 March 2017 / Published online: 26 May 2017

© Shanghai Institute of Applied Physics, Chinese Academy of Sciences, Chinese Nuclear Society, Science Press China and Springer Science+Business Media Singapore 2017

Abstract Besides the original seeded undulator line, in the soft X-ray free-electron laser (SXFEL) user facility in Shanghai, a second undulator line based on self-amplified spontaneous emission is proposed to achieve 2-nm laser pulse with extremely high brightness. In this paper, the beam energy deviation induced by the undulator wakefields is numerically calculated, and 3D and 2D results agree well with each other. The beam energy loss along the undulator degrades the expected FEL output performances, i.e., the pulse energy, radiation power and spectrum, which can be compensated with a proper taper in the undulator. Using the planned time-resolved diagnostic, a novel experiment is proposed to measure the SXFEL longitudinal wakefields.

Keywords SXFEL · Wakefields · Pulse energy · Radiation power · Spectrum · Taper

1 Introduction

The invention of free-electron laser (FEL) provides the cutting-edge scientific technique in various fields, ranging from unveiling chemical dynamics to probing surface

catalysis, and from material sciences to medical physics [1, 2]. Nowadays, more and more X-ray FEL facilities are under construction and operation all over the world, such as LCLS [3, 4] and FLASH [5], which generate extremely ultrashort-pulse and high-intensity radiation. China's first X-ray FEL is under construction in Shanghai, namely SXFEL test facility [6]. To extend the SXFEL wavelength down to water window region of 2 nm, a user facility is proposed, as shown schematically in Fig. 1.

On the basis of the test facility, four more C-band accelerators will be installed in the reserved Linac space. They will accelerate the electron beam from 0.84 to 1.5 GeV. Thus, with the additional seven undulator segments, the baseline seeded FEL scheme of test facility, i.e., two-stage of high-gain harmonic generation (HG) [7] and echo-enabled harmonic generation (EEHG) [8], will achieve 3 nm wavelength. Meanwhile, to fully cover the water window wavelength, an extracted FEL branch operated in self-amplified spontaneous emission (SASE) [9] mode will be built, which simply consists of the undulator segments and insert transitions.

SXFEL aims to produce high-brightness photon pulse with narrow bandwidth, but the designed FEL pulse may degrade due to negative wakefield effects along the SXFEL undulator section. Thus, it is necessary to calculate wakefields in the undulator chambers and other impedance items, so as to evaluate the FEL performance, e.g., the pulse energy and FEL bandwidth. An intensive study of longitudinal wakefields and its effects on seeded FEL branch outputs for SXFEL test facility has been carried out [10], under Gaussian beam profile assumption. More recently, analytical descriptions and 2D computations of wakefields have been preliminarily considered for SXFEL user facility [11].

This work was supported by the National Natural Science Foundation of China (Nos. 11475250 and 11322550) and Ten Thousand Talent Program.

✉ Hai-Xiao Deng
denghaixiao@sinap.ac.cn

¹ Shanghai Institute of Applied Physics, Chinese Academy of Sciences, Zhangjiang Campus, Shanghai 201204, China

² University of Chinese Academy of Sciences, Beijing 100049, China

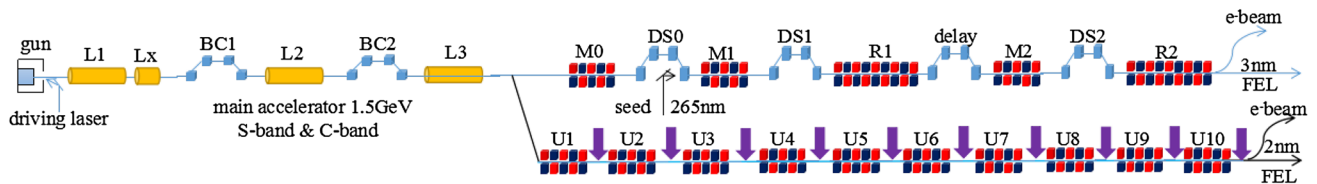
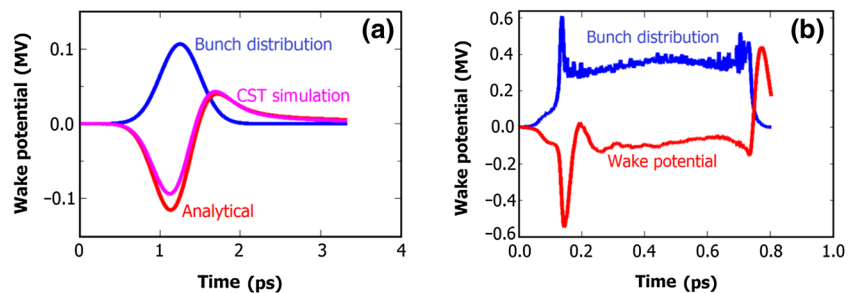


Fig. 1 (Color online) Layout of SXFEL user facility consists of seeded and SASE branches

Fig. 2 (Color online) Resistive wall wakefield (a) by theoretical analysis and CST simulation and the wake potential (b) under the real bunch profile



The electron beam quality degradations due to wakefields during the phases of acceleration, bunch compression, transportation, have important electromagnetic effects on the FEL process; thus, wakefields are extensively investigated in FERMI [12–14], European XFEL [15], PAL-XFEL [16], SACLA [17] and LCLS [18]. In general, the wakefields calculation relies on analytical formulas and numerical codes. For the SASE branch of SXFEL user facility, apart from the undulator vacuum chamber, there are 10 inserted pipes with round cross section that connect each undulator. Therefore, it is necessary to check the 3D effects of the wake calculations in those irregular structures, e.g., flat vacuum chamber and rectangular-to-round step-out. Thus, numerical calculations are carried out with 3D computer solver CST particle studio [19].

In practice, when using the simulation code like ABCI [20] and CST particle studio, only the Gaussian bunch shape can be involved, rather than a real distribution. In this paper, the wakefields generated in the resistive wall and the discontinuities of beam pipe are considered for SXFEL user facility, under the real beam profile tracked with ELEGANT [21], and the 3D and 2D wakefields calculation results are compared. Considering the FEL lasing process, usually the wakefield itself and the FEL performances are studied separately. Unlike the traditional way, the whole undulator system is divided into modules for wakefield calculation; then, the wakefield impact is imported timely and locally on the electron beam. The results show that the pulse energy of the final 2-nm FEL pulse will be degraded by a factor of 7.5 with a gradual beam energy loss of 4 MeV along the whole undulator section, but this can be compensated by a fine tuning of the

undulator taper. Finally, using the recently developed transverse deflector technique [22, 23], a proof of principle wakefields measurement at SXFEL user facility is proposed.

2 Wakefields calculation

In SXFEL user facility, the linear accelerator provides 1.5-GeV electron beam in 500 pC bunch charge and 50 Hz repetition rate; thus, the wakefields considered here are limited in the head–tail wake. For the SASE beamline of SXFEL user facility, 10 in-vacuum undulators will be used to reach the target wavelength. Then, the electron beam should pass through the space between two opposite magnetic poles, which can be treated as flat vacuum chamber. Therefore, the short-range resistive wall effect that arose from metallic wall can be calculated [24, 25]. The vacuum chamber, with complex surface as observed under atomic microscopy [26], can be accurately modeled in simulations. However, the surface roughness wake [27, 28] appears relatively small. Thus in CST simulation, the resistive wall is simply regarded as a smooth surface, and a Gaussian beam current is considered due to the limitation of CST wakefield solver.

Figure 2a shows the resistive wall potentials for one undulator segment given by CST and analytical theory. The two results are consistent with each other despite a slight deviation. For a Gaussian distribution with FWHM pulse duration of 250 fs, here, the mean beam energy losses due to resistive wall are 59.5 keV by CST simulation and 44.2 keV from the theory. In order to evaluate the final

FEL performance at the end of undulator section, a wakefield calculation with real beam profile is needed to obtain the real energy loss. From Fig. 2b, the mean energy loss from the resistive wall in single undulator segment is approximately 106 keV.

It seems that the SASE undulator line is slightly simpler in configuration than the seeded undulator line [11]. However, the beam position monitors, profile monitors, quadruples and correctors between undulator segments are still required to adjust the electron beam trajectory. Thus, the undulators need to be interrupted and connected by these transitions. Studies on 2D Geometric wakefield have been done [10, 11] using the ABCI [20]. Generally, ABCI is 2D calculation software. It employs a moving mesh that encloses the longitudinal and transverse direction, and deals with, strictly speaking, cylindrical symmetric structures only. Differently, CST is an indirect integration method [29] to handle 3D arbitrary structures, but it needs great computation abilities. Thus due to the limitation of ABCI, CST wakefield calculation of interaction between discontinuities and electron beam will be revealed here.

However, by comparing the CST and ABCI simulations under Gaussian distribution, the results of flange, profile monitor and step-out are almost the same, with their mean beam energy losses being 0.12, 1.12 and 77.06 keV, respectively, on the basis of Fig. 3 (the beam energy loss due to step-out is dominant). The undulator transition in

SXFEL user facility consists of flanges, bellows, profile monitor, step-out and step-in; thus, the wakefield should be obtained accurately by simulating the whole transition under the CST interface, rather than separate calculations. However, the calculated meshes will increase dramatically to several billions when applying for an ultrashort bunch like the SXFEL user facility. Due to the limitation in computation ability, the whole 3D structure wakefield computation can be replaced by 2D ABCI simulation. Figure 4a plots the ABCI wakefield results of undulator transition with the real bunch profile, with the mean energy loss of 264.8 keV. A single undulator wakefield and a transition wakefield are calculated under the real bunch profile. The total energy deviation is approximately 4 MeV (Fig. 4b), obtained through a superposition of several modules.

3 Wakefield impact on photon pulse

Considering the wakefield effects in the undulator system, once the sliced beam energy loss becomes comparable to the pierce parameter, most electrons will not satisfy the resonant condition again, leading to low FEL efficiency and gain reduction. Generally, the FEL reduction caused by the continuous beam energy loss can be compensated by gradually tapering the undulator to sustain the interaction

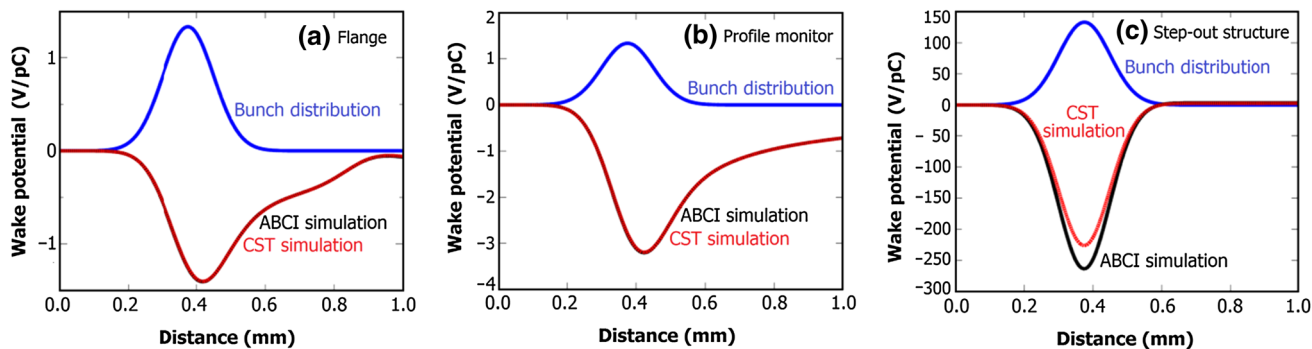
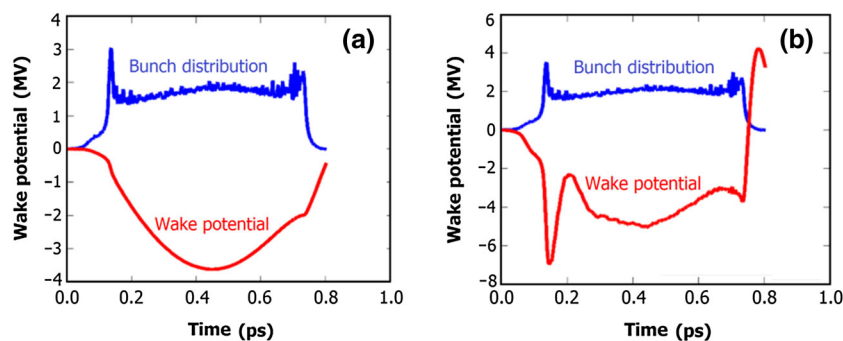


Fig. 3 (Color online) Comparison of the wake potentials obtained by ABCI and CST simulations

Fig. 4 (Color online) Wake potential of undulator transition with the real bunch profile (a) and the total wake potential of SASE undulator section (b)



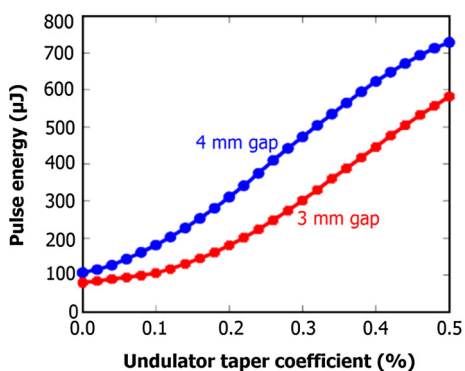


Fig. 5 (Color online) FEL pulse energy vs undulator taper coefficient, by a start-to-end SASE simulation, with the same random seed for all the SASE runs

even when the electrons lose a large fraction of their energy. Undulator tapering technique has been investigated since early days of FEL technology when FEL was proposed to produce very high power [30, 31]. In this paper, only the linear taper of SXFEL undulator is discussed, defined as

$$K(z) = K_0(1 - g)\frac{z}{L}, \tag{1}$$

where K_0 is the initial undulator parameter, L is the total length of undulator and g is the linear taper coefficient.

To model the expected SASE FEL performance of SXFEL user facility, start-to-end simulation is used to evaluate the wakefield effects and the compensation

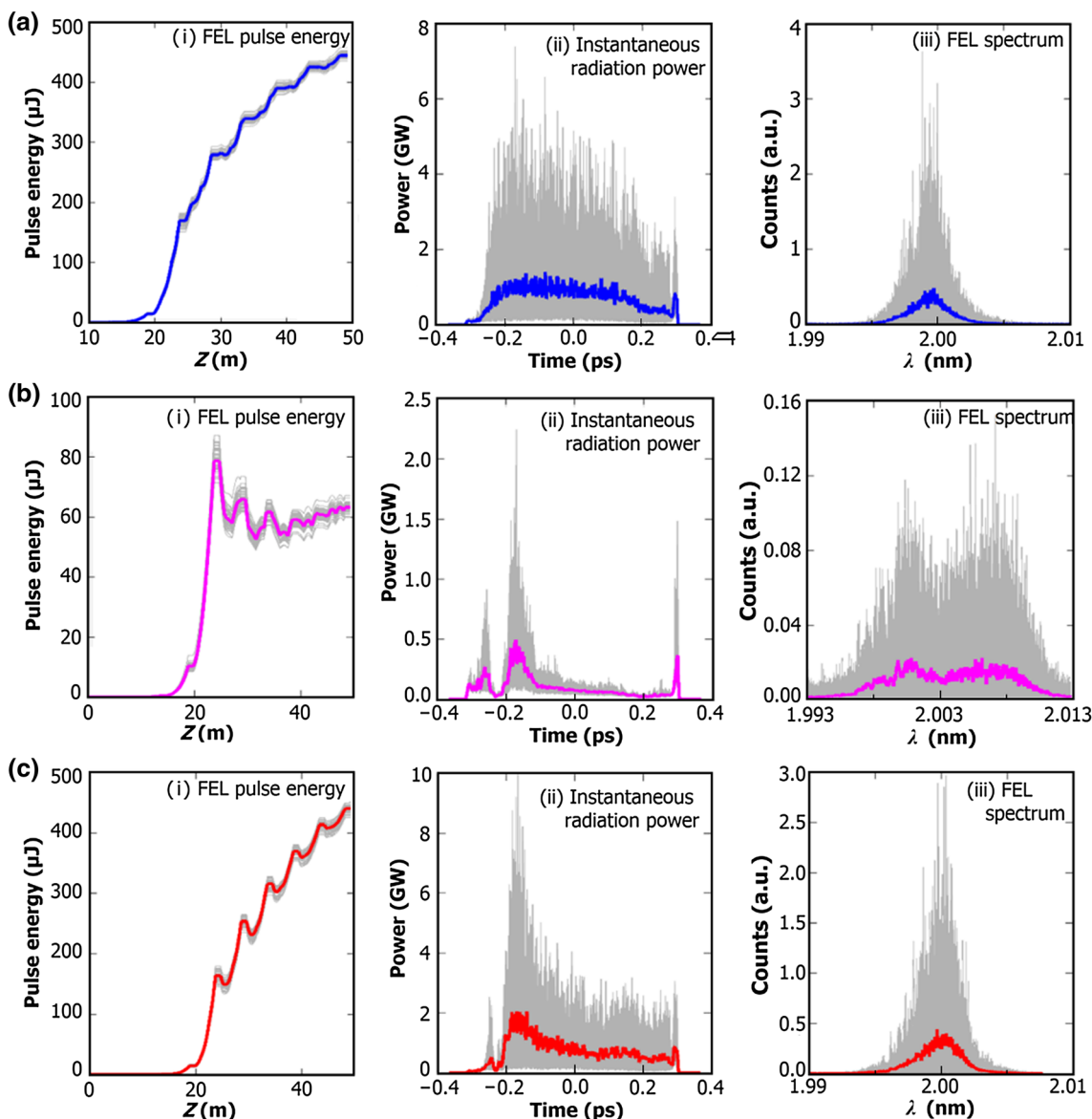


Fig. 6 (Color online) Pulse energy evolution vs undulator section, radiation power distribution vs time and spectral domain, without (a) and with (b) wakefield effects, and with the undulator taper technique at $g = 0.4\%$

strategy using taper undulator technique. At the exit of the undulator, the simulated 2-nm pulse energy without wake effects is 447 μJ . Figure 5 shows the FEL pulse energy dependence on the taper coefficient when the wakefields are applied in the simulation. Considering different magnet options for satisfying the required fields of in-vacuum undulator, undulator gaps of 3 and 4 mm are used. Although a larger undulator gap contributes to a lower wakefields effects on FEL performances, the 3-mm gap is studied in next sections to estimate the worst case. From Fig. 5, one finds that the pulse energy at the exit of tapered undulator section can be several times larger than the untapered cases, and the FEL pulse energy achieves 447 μJ at $g = 0.4\%$. This is a limit of the tapering coefficient, above which the FEL pulse energy increase will be beyond the topic of this paper.

In order to avoid the shot-to-shot fluctuation of SASE FEL, 50-shot simulations with different shot noise are carried out. Figure 6 shows the FEL pulse energy evolution, instantaneous radiation power and FEL spectrum at the exit of the undulator section. In the absence of the wakefield-induced energy losses (Fig. 6a), the 2-nm FEL can finally achieve 450 μJ pulse energy with a peak power of approximately 1 GW. However, when the wakefield is considered (Fig. 6b), the FEL pulse energy drops to 63 μJ and the spectrum degrades and broadens. With an undulator taper coefficient of 0.4% (Fig. 6c), it is deserved to note that FEL pulse energy, radiation power and spectrum can be approximately retrieved to those without wakefield.

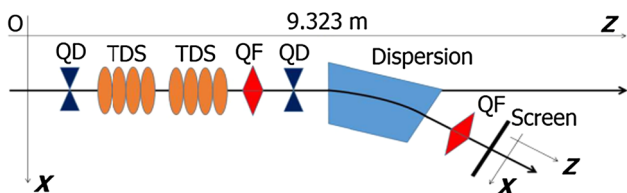


Fig. 7 (Color online) Layout of the transverse deflector beamline downstream the undulator section

4 Proposed wakefield measurement

Wakefields are frequently considered in beam control and accelerator operation. The wakefield measurement has been difficult in circular machine for many years. It is now equally important for the FEL facility due to stringent requirement of extremely high-brightness beam. Among the techniques developed to measure and diagnose bunch profile with high temporal resolution (including zero RF phasing and streak camera), transverse deflectors are widely used for time-resolved beam energy, emittance and radiation profile measurements in modern FEL facilities [22, 23].

As shown in Fig. 7, a transverse deflector beamline downstream the undulator is designed for SXFEL user facility. Four quadruples are used from beam optics optimization and the bending magnet is used for beam momentum and spread measurement. The transverse deflector then provides the abilities to measure the longitudinal phase space of the electron beam with a temporal resolution of 6.6 fs [32]. Apart from it, the method to reconstruct the whole longitudinal wakefield that arose from the undulator section is also possible, because that alterable gap in-vacuum undulators are used.

The procedure to retrieve the undulator wake potential distribution is as follows. Generally, when all the undulator gaps are open, the longitudinal phase space retrieved at the exit of undulator does not take wakefield into account (Fig. 8a); when the undulator gap is closed, the longitudinal phase space on the observation screen at the exit of undulator takes wakefields into account (Fig. 8b). By subtracting the beam energy of Fig. 8a from Fig. 8b, we can obtain the wake potential in Fig. 8c, which shows a good agreement between the simulated wake and the reconstructed one. Besides, since the beam current profile can be characterized by the transverse deflector, the wake function and the mean beam energy loss can be deduced in such a measurement experiment. We note that the undulators should be set at slightly different gaps to disturb the

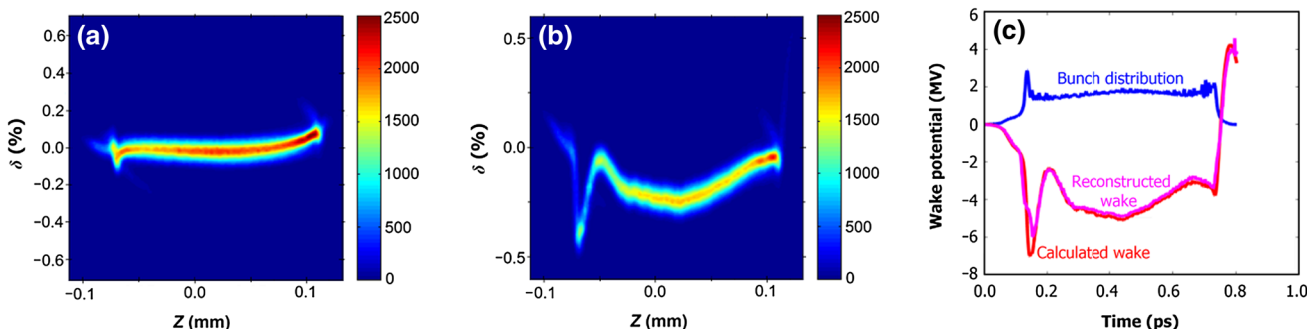


Fig. 8 (Color online) Reconstructed longitudinal phase space of the electron beam without (a) and with (b) undulator wake effects, and the reconstructed undulator wake potential (c) obtained by subtracting the beam energy in b from a

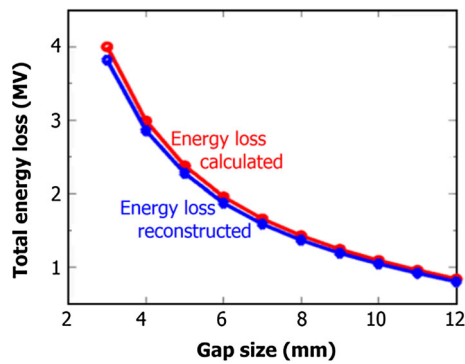


Fig. 9 (Color online) Calculated beam energy loss and the reconstructed one with different undulator gaps

FEL resonance and thus avoid lasing during all the measurement, and then, the beam energy loss induced by FEL lasing can be neglected in above-mentioned procedures.

The above results are from an undulator gap of 3 mm. The gap size effects on final wakefields are studied by calculating the total beam energy losses with undulator gaps of 3–12 mm. Obviously, the induced energy deviations will experience a descending trend with the increasing gap size; for instance, the energy loss is approximately 1 MeV when the gap is 12 mm, which is a quarter of the 3 mm case and has slight impact on the FEL performance. Also, to examine the accuracy of the proposed measurement, the computed and reconstructed energy losses are compared in Fig. 9. They are close to each other.

5 Conclusion

Generally, on account of the relative long electron bunch and simple accelerating structure, wakefield effects in the linear accelerator is small and more importantly could be compensated with the help of feedback system. Therefore, in this paper, an accurate 3D wakefields calculation using the CST particle studio is accomplished for the resistive wall and geometric discontinuities of undulator sections in SXFEL user facility. It is demonstrated that there is a reasonable agreement between the 3D and 2D results. Moreover, in the start-to-end FEL simulation with the wakefields effects, the total beam energy loss of 4 MeV along the undulator section causes a serious degradation of FEL performance; for example, the pulse energy drops to 63 μ J from original 450 μ J. Fortunately, the FEL performance loss caused by wakefields can be compensated with an undulator taper of 0.4%. Also, in the SXFEL user facility, the longitudinal wakefields measurement and calibration can be accomplished with the planned time-resolved diagnostics. In the simulation, the reconstructed wake potential has a good agreement with the theoretical

one. More simulations and experiments will be carried out in the future to help understand the longitudinal wakefields in modern FEL facilities.

Acknowledgements The authors are grateful to Xiao Hu, Wei Zhang, Meng Zhang, Kai Li and Han Zhang for helpful discussions and useful comments.

References

1. W.A. Barletta, J. Bisognano, J.N. Corlett et al., Free electron lasers: present status and future challenges. *Nucl. Instrum. Methods Phys. Res. A* **618**, 69–96 (2010). doi:[10.1016/j.nima.2010.02.274](https://doi.org/10.1016/j.nima.2010.02.274)
2. H. Öström, H. Öberg, H. Xin et al., Probing the transition state region in catalytic CO oxidation on Ru. *Science* **347**, 978–982 (2015). doi:[10.1126/science.1261747](https://doi.org/10.1126/science.1261747)
3. P. Emma, R. Akre, J. Arthur et al., First lasing and operation of an ångstrom-wavelength free-electron laser. *Nat. Photonics* **4**, 641–647 (2010). doi:[10.1038/nphoton.2010.176](https://doi.org/10.1038/nphoton.2010.176)
4. T. Ishikawa, H. Aoyagi, T. Asaka et al., A compact X-ray free-electron laser emitting in the sub-ångström region. *Nat. Photonics* **6**, 540–544 (2012). doi:[10.1038/nphoton.2012.141](https://doi.org/10.1038/nphoton.2012.141)
5. W. Ackermann, G. Asova, V. Ayvazyan et al., Operation of a free-electron laser from the extreme ultraviolet to the water window. *Nat. Photonics* **1**, 336–342 (2007). doi:[10.1038/nphoton.2007.76](https://doi.org/10.1038/nphoton.2007.76)
6. Shanghai soft X-ray free-electron laser test facility conceptual design report. Shanghai Institute of Applied Physics, Chinese Academy of Sciences, Shanghai (2015)
7. L.H. Yu, Generation of intense UV radiation by subharmonically seeded single-pass free-electron lasers. *Phys. Rev. A* **44**, 5178–5193 (1991). doi:[10.1103/PhysRevA.44.5178](https://doi.org/10.1103/PhysRevA.44.5178)
8. G. Stupakov, Beam echo effect for generation of short-wavelength radiation. *Phys. Rev. Lett.* **102**, 074801 (2009). doi:[10.1103/PhysRevLett.102.074801](https://doi.org/10.1103/PhysRevLett.102.074801)
9. A. Kondratenko, E. Saldin, Generation of coherent radiation by a relativistic-electron beam in an undulator. *Part. Accel.* **10**, 207–216 (1980)
10. M. Song, K. Li, C. Feng et al., Wakefield issue and its impact on X-ray photon pulse in the SXFEL test facility. *Nucl. Instrum. Methods Phys. Res. A* **822**, 71–76 (2015). doi:[10.1016/j.nima.2016.03.089](https://doi.org/10.1016/j.nima.2016.03.089)
11. M. Song, H. Deng, C. Feng et al., Longitudinal wakefields in the undulator section of SXFEL user facility, in *Proceedings of IPAC16, Busan, Korea, MOPOR005*, pp. 595–597
12. A. Lutman, *Impact of the wakefields and of an initial energy curvature on a Free Electron Laser*. Ph.D. thesis, Università Degli Studi Di Trieste (2010)
13. P. Craievich, *Short-range longitudinal and transverse wakefield effects in FERMI@Elettra FEL project*. Ph.D. thesis, Technische Universiteit Eindhoven (2010)
14. FERMI@Elettra Concept Design Report, Trieste (2007)
15. I. Zagorodnov, T. Weiland, The short-range transverse Wakefields in Tesla accelerating structure, in *Proceedings of PAC03, Portland, Oregon, USA, RPPG034*, pp. 3249–3251
16. T.Y. Lee, H.S. Kang, J. Choi, Study of PAL-XFEL wake field effects with the GENESIS code, in *Proceedings of FEL05, Stanford, California, USA, THPP024*, pp. 502–505
17. T. Tanaka, S. Goto, T. Hara et al., Undulator commissioning by characterization of radiation in X-ray free electron lasers. *Phys. Rev. Spec. Top. Accel. Beams* **15**, 110701 (2012). doi:[10.1103/PhysRevSTAB.15.110701](https://doi.org/10.1103/PhysRevSTAB.15.110701)

18. K. Bane, I. Zagorodov, Wakefields in the LCLS Undulator Transitions, in *Proceedings of EPAC06, Edinburgh, Scotland, THPCH072*, pp. 2952–2954
19. CST-computer simulation technology. <http://www.cst.de/>
20. ABCI Home Page. <http://abci.kek.jp/abci.htm>
21. M. Borland, Elegant: a flexible SDDS-compliant code for accelerator simulation. Adv. Photon Source LS-287 (2000)
22. R. Akre, L. Bentson, P. Emma et al., A transverse RF deflecting structure for bunch length and phase space diagnostics, in *Proceedings of PAC01, Chicago, IL, USA, WPAH116*, pp. 2353–2355
23. Y. Ding, F.J. Decker, V.A. Dolgashev et al., *Results from the LCLS X-Band transverse deflector with femtosecond temporal resolution* (SLAC National Accelerator Laboratory, USA, SLAC-PUB-16015, 2014)
24. K. Bane, G. Stupakov, Using surface impedance for calculating wakefields in flat geometry. Phys. Rev. Spec. Top. Accel. Beams **18**, 034401 (2015). doi:[10.1103/PhysRevSTAB.18.034401](https://doi.org/10.1103/PhysRevSTAB.18.034401)
25. K. Bane, G. Stupakov, *Roughness tolerance studies for the undulator beam pipe chamber of LCLS-II* (SLAC National Accelerator Laboratory, USA, SLAC-PUB-15951, 2014)
26. G. Stupakov, Surface roughness impedance. AIP Conf. Proc. **581**, 141–152 (2001). doi:[10.1063/1.1401569](https://doi.org/10.1063/1.1401569)
27. G. Stupakov, R.E. Thomson, D. Walz et al., Effects of beam-tube roughness on X-ray free electron laser performance. Phys. Rev. Spec. Top. Accel. Beams **2**, 060701 (1999). doi:[10.1103/PhysRevSTAB.2.060701](https://doi.org/10.1103/PhysRevSTAB.2.060701)
28. G. Stupakov, Impedance of small obstacles and rough surfaces. Phys. Rev. Spec. Top. Accel. Beams **1**, 064401 (1998). doi:[10.1103/PhysRevSTAB.1.064401](https://doi.org/10.1103/PhysRevSTAB.1.064401)
29. I. Zagorodnov, Indirect methods for wake potential integration. Phys. Rev. Spec. Top. Accel. Beams **9**, 102002 (2006). doi:[10.1103/PhysRevSTAB.9.102002](https://doi.org/10.1103/PhysRevSTAB.9.102002)
30. W.M. Fawley, Z. Huang, K.J. Kim et al., Tapered undulators for SASE FELs. Nucl. Instrum. Methods Phys. Res. A **483**, 537–541 (2002). doi:[10.1016/S0168-9002\(02\)00377-7](https://doi.org/10.1016/S0168-9002(02)00377-7)
31. Y. Jiao, J. Wu, Y. Cai et al., Modeling and multidimensional optimization of a tapered free electron laser. Phys. Rev. Spec. Top. Accel. Beams **15**, 050704 (2012). doi:[10.1103/PhysRevSTAB.15.050704](https://doi.org/10.1103/PhysRevSTAB.15.050704)
32. M. Song, H. Deng, B. Liu et al., Deflecting cavity considerations for time-resolved machine studies of SXFEL user facility, in *Proceedings of IBIC16, Barcelona, Spain, MOPG50*, pp. 169–172